

Luminescent Tetranuclear Copper(I) and Gold(I) Heterobimetallic Complexes: A Phosphine Acetylide Amidinate Orthogonal Ligand Framework for Selective Complexation

Shubham,^[a] Vanitha R. Naina,^[a] and Peter W. Roesky^{*[a, b]}

The synthesis of phosphine acetylide amidinate stabilized copper(I) and gold(I) heterobimetallic complexes was achieved by reacting ligand $[\{\text{Ph}_2\text{PC}\equiv\text{CC}(\text{NDipp})_2\}\text{Li}(\text{thf})_3]$ (Dipp = 2,6-N,N'-diisopropylphenyl) with CuCl and Au(tht)Cl, yielding the eight membered ring $[\{\text{Ph}_2\text{PC}\equiv\text{CC}(\text{NDipp})_2\}_2\text{Cu}_2]$ and the twelve membered ring $[\{\text{Ph}_2\text{PC}\equiv\text{CC}(\text{NDipp})_2\}_2\text{Au}_2]$. $\{\text{Ph}_2\text{PC}\equiv\text{CC}(\text{NDipp})_2\}_2\text{Cu}_2]$ features a Cu_2 unit, which is bridged by two amidinate ligands, served as a metalloligand to synthesize the heterobimetallic Cu^I/Au^I complexes $[\{(\text{AuX})\text{Ph}_2\text{PC}\equiv\text{CC}(\text{NDipp})_2\}_2\text{Cu}_2]$ ($\text{X}=\text{Cl}, \text{C}_6\text{F}_5$).

In these reactions, the central ring structure is retained. In contrast, when the twelve membered ring $[\{\text{Ph}_2\text{PC}\equiv\text{CC}(\text{NDipp})_2\}_2\text{Au}_2]$ was reacted with CuX ($\text{X}=\text{Cl}, \text{Br}, \text{I}$ and Mes), the reaction led to the rearrangement of the central ring structure to give $[\{(\text{AuX})\text{Ph}_2\text{PC}\equiv\text{CC}(\text{NDipp})_2\}_2\text{Cu}_2]$ ($\text{X}=\text{Cl}, \text{Br}, \text{I}$ and Mes), which feature the same the eight membered Cu_2 ring as above. These compounds were also synthesized by a one-pot reaction. The luminescent heterobimetallic complexes were further investigated for their photophysical properties.

Introduction

In recent years, there has been a surge of interest in the synthesis of heterobimetallic complexes owing to their potential applications in various fields such as catalysis,^[1–2] optoelectronics^[3] as well as medical applications.^[4–5] These complexes are unique metal compounds that feature two different metal atoms bonded within a single molecular entity.^[6–7] Their growing popularity can be attributed to the combination of distinct properties of the two metal atoms, including differences in size, valence shell, and hard-soft acid-base affinities, among others. Cooperativity between the metal centres in combination with a judicious choice of ligand framework, often leads to molecular architectures with distinct properties which cannot be harnessed with their monometallic counterparts.^[8]

Depending on the type of metals used, heterobimetallic complexes also exhibit photoluminescence (PL) properties.^[9–11] Luminescent heterobimetallic complexes are majorly developed using coinage metals because of their fully-filled d^{10} electronic

configuration and the absence of low-lying metal-centred excited states.^[12] Cu^I and Au^I have different affinities towards soft and hard donor atoms due to “hard and soft acids and bases” (HSAB) interactions.^[13–15] Researchers have exploited this property and designed several orthogonal ligand scaffolds which can selectively coordinate to copper(I) and gold(I) metal centres.^[16–23] A combination of amidinate and phosphine functional groups with N- and P- donor groups, is one of the interesting orthogonal ligand frameworks to access tailored heterobimetallic complexes.^[24–27]

Coinage metal complexes in +1 oxidation state ligated by amidinate ligands are known to form dimeric complexes of the form “ L_2M_2 ” ($\text{M}=\text{Cu}, \text{Ag}, \text{Au}$) and this kind of network is maintained by attractive metal-to-metal interactions.^[23,29] These types of attractive forces typically observed for d^{10} metals are termed as metallophilic interactions.^[30–39] Metal complexes with such interactions have rich photophysical properties due to the alteration of a ligand to metal charge transfer (LMCT) transition in a mononuclear complex to a ligand to metal–metal charge transfer (LMMCT) transition in a binuclear complex, resulting in a smaller HOMO-LUMO gap.^[38,40–41]

There are handful examples of Cu^I amidinates of the type $[(\text{R}'\text{NC}(\text{R})\text{NR}'')\text{Cu}]_2$ (R' and $\text{R}''=n$ -propyl, isopropyl, n -butyl, i -butyl, sec -butyl, t -butyl; $\text{R}=\text{methyl}, n$ -butyl) disclosed by Gordon *et al.*, where they demonstrated that these compounds exist in the form of planar dimers, bridged by nearly linear N–Cu–N bonds and these complexes were used for atomic layer deposition.^[42] Similar dinuclear Cu^I and Ag^I amidinate complexes were synthesized by Walensky *et al.* in 2014 where they studied the reactivity of these compounds with CS_2 to form Cu_4S_8 clusters^[43] and later, they synthesized di- and trinuclear mixed-valent copper complexes by the reduction of Cu^I amidinate complex with iodine.^[44] There are some examples of Cu^I complexes with zwitterionic imidazolium-2-amidinate,

[a] Shubham, Dr. V. R. Naina, Prof. Dr. P. W. Roesky
Institute of Inorganic Chemistry
Karlsruhe Institute of Technology
Kaiserstr.12, 76131 Karlsruhe (Germany)
E-mail: roesky@kit.edu

[b] Prof. Dr. P. W. Roesky
Institute of Nanotechnology (INT)
Karlsruhe Institute of Technology,
Kaiserstr.12, 76131 Karlsruhe (Germany)

Supporting information for this article is available on the WWW under <https://doi.org/10.1002/chem.202401696>

© 2024 The Authors. Chemistry - A European Journal published by Wiley-VCH GmbH. This is an open access article under the terms of the Creative Commons Attribution License, which permits use, distribution and reproduction in any medium, provided the original work is properly cited.

which is an electroneutral amidinate ligand.^[28] In 2018, the synthesis of dodecacopper(I) extended metal atom chains supported by hexadentate bis(pyridylamido)amidinate were reported.^[45] Moreover, there have been examples of phosphoamidate Cu^I complexes and clusters^[46–49] and there are multinuclear Cu^I/Ag^I complexes in the literature with coumarin functionalized aminodiphosphine ligand.^[50]

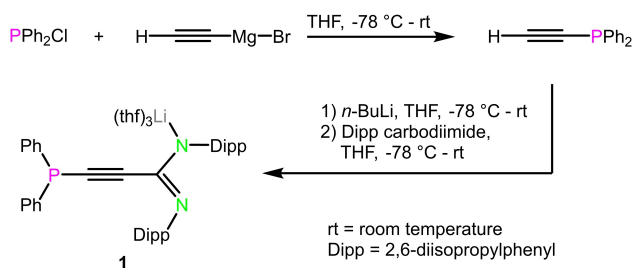
Gold(I) complexes^[51] comprised of alkyne functionalized amidinate were disclosed by our group previously. Here, the synthetic potential of alkynyl groups for the formation of multimetallic structures was investigated.^[52] The alkynyl moiety is of great interest as it is often involved in photophysical processes of organometallic compounds by the metal to ligand charge transfer to the $\pi^*(C\equiv C)$ orbitals and radiative relaxation could also occur after the photoexcitation.^[53–54] Later in 2021, PNNP based ligand *N,N'*-bis[(2-diphenylphosphino)phenyl]-formamidinate (dpfam[−]) has been used for the site specific coordination of N and P centres to Cu^I and Au^I, respectively, and all of them were observed to be luminescent.^[55–57]

Herein, we report a phosphine substituted acetylide amidinate ligand containing an alkynyl moiety and a phosphine centre. The efficiency of this ligand for the synthesis of heterobimetallic complexes of Cu^I and Au^I both in a stepwise manner and one-pot reaction was investigated. These complexes differ from each other in terms of coordination modes and coordinating ligand at the Au^I centre. Further, the complexes were studied in terms of their photophysical properties.

Results and Discussion

Synthesis and Characterization

The phosphine substituted lithium acetylide amidinate (1) was obtained in a two-step protocol (Scheme 1). The first step involves the synthesis of diphenylphosphine substituted acetylene (Ph₂PC≡CH), which was isolated from the reaction of chlorodiphenylphosphine (Ph₂PCl) with ethynyl magnesium bromide (HC≡CMgBr) in a 1:1.1 ratio, respectively, in tetrahydrofuran (THF) at −78 °C (Scheme 1).^[58] This step is followed by deprotonation of Ph₂PC≡CH using *n*-BuLi (1.1 eq.), and further reaction was performed with *N,N'*-2,6-diisopropylphenyl carbodiimide (Dipp carbodiimide), which afforded the desired lithium



Scheme 1. Synthesis of lithium salt of phosphine substituted lithium acetylide amidinate (1).

salt of phosphine substituted acetylide amidinate ligand **1** in a quantitative yield (Scheme 1).

Compound **1** was characterised by single crystal X-ray diffraction (SC-XRD) (Figure 1), NMR and IR spectroscopy as well as elemental analysis. From the molecular structure of **1** obtained by SC-XRD, it was found to be a monomer crystallizing in the monoclinic space group (*P*2₁/*n*). The Li ion is four-fold coordinated by one nitrogen atom of the amidinate ligand and three molecules of THF. This can also be ensured by the resonances at $\delta = 1.29$ and 3.55 ppm in the ¹H NMR spectrum of **1**. The characteristic resonance for **1** in the ³¹P{¹H} NMR spectrum was observed at $\delta = -33.6$ ppm. In addition, C≡C stretching absorption band in the IR spectrum was detected at 2165 cm^{−1}.

The Li–N1 bond length is found to be 1.989(2) Å, which is in agreement with previously reported Li–N bond length in [(Me₃SiC≡CC(NDipp)₂Li(thf)₃] (2.009(6) Å).^[52]

The obtained ligand was further investigated for its coordination behaviour towards copper(I) and gold(I) precursors. Compound **1** was reacted with CuCl in an equimolar ratio at room temperature, which afforded the formation of desired copper amidinate complex [(Ph₂PC≡CC(NDipp)₂Cu]₂ (**2**) in almost quantitative yield (Scheme 2). After filtration and drying, analytically pure compound **2** was obtained as a light-yellow coloured powder.

Although single crystals for compound **2** could not be obtained, the molecular ion peak at *m/z* = 1268.5018 in the ESI-MS spectrum in addition to other standard characterization, confirms the successful synthesis. In the ¹H NMR spectrum, the methine protons of the Dipp moiety displayed an upfield shift from $\delta = 3.78$ ppm (**1**) to $\delta = 3.47$ ppm (**2**). The resonances of the *i*-Pr methyl protons appear as two doublets at $\delta = 1.14$ and 1.06 ppm rather than a single resonance at $\delta = 1.40$ ppm, which was observed for **1**. Additionally, in the ³¹P{¹H} NMR spectrum,

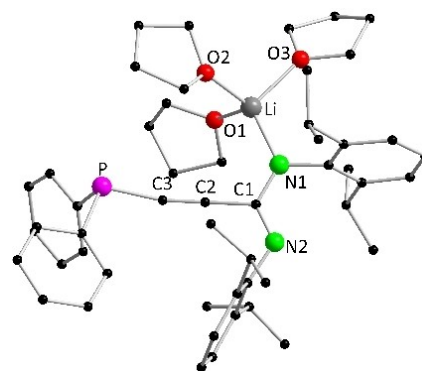
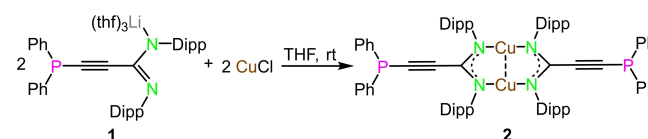


Figure 1. Molecular structure of **1** in the solid state. Hydrogen atoms are omitted for clarity. Structural parameters are given in the ESI (Figure S43).



Scheme 2. Synthesis of copper(I) amidinate complex **2**.

the resonance is downfield shifted to $\delta = 19.9$ ppm when compared to the precursor ligand **1** ($\delta = -33.6$ ppm). Upon excitation with UV light, compound **2** exhibits a vibrant greenish-yellow luminescence.

Two different attempts to synthesize the Au analogue of compound **2** resulted in an unprecedented twelve membered ring structure **3** (Scheme 3). In the first approach (Route A, Scheme 3) the lithium salt **1** was reacted with Au(tht)Cl (tht = tetrahydrothiophene) in THF at room temperature to give complex **3** in 74% yield (Scheme 3). In the second approach (Route B, Scheme 3), complex **3** can also be synthesized by starting from the previously reported Au^I acetylene complex (**4**).^[54] Using 2.1 eq. of *n*-BuLi in THF for the deprotonation. Followed by subsequent reaction with PPh₂Cl gave a rearrangement reaction complex **3** as the final product in 67% yield. This method provided an unexpected but alternative route for the synthesis of complex **3**, offering flexibility in the preparation of this compound.

The molecular structure of **3** in the solid state was elucidated using SC-XRD analysis and it features a 12-membered ring with P–Au–N bonding. The affinity of Au^I towards soft donor atoms led to the rearrangement and formation of the 12-membered ring, wherein each Au^I atom is coordinated to one phosphine and one nitrogen atom from two different amidinate moieties in a linear geometry with a P–Au–N1 angle of 177.8(10)°. The Au–N and Au–P bond distances are 2.027(3) Å and 2.215(10) Å, respectively. These bond distances are in good agreement with the ones reported for [((PPh₃)AuC≡CC(NDipp))₂Au₂], i.e. 2.020(6) Å and 2.272(2) Å for Au–N and Au–P bonds, respectively.^[54] Additionally, the non-equivalency of the two C–N bonds was confirmed by their respective bond lengths. The C1–N1 bond length of 1.337(5) Å indicates a single bond character, while C1–N2 bond length was found to be 1.289(5) Å, confirming its nature as a double bond.

Analysis of the ¹H NMR spectrum revealed two distinct sets of signals for the two non-equivalent Dipp moieties present in the molecule. Specifically, a septet at $\delta = 3.21$ ppm was observed for the proton of the Dipp groups attached to N1 (Figure 2), while another septet at $\delta = 3.71$ ppm corresponded to the Dipp groups attached to the carbon doubly bonded to N2.

In the ³¹P{¹H} NMR spectrum, a significant shift was observed, transitioning from $\delta = -33.6$ ppm (**1**) in the starting material to $\delta = 2.1$ ppm (**3**). The rearrangement of the Au^I atoms from complex **4** to complex **3** led to the loss of aurophilic

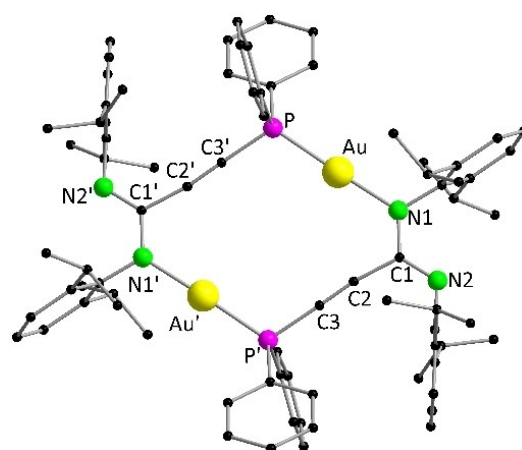


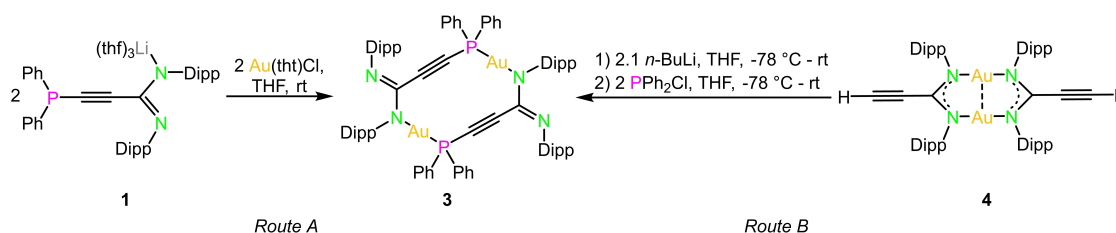
Figure 2. Molecular structure of **3** in the solid state. Hydrogen atoms and non-coordinating solvents are omitted for clarity. Structural parameters are given in the ESI (Figure S44).

interactions which might be attributed to the non-emissive nature of complex **3**.

In the next step, we were interested in using compound **2** as a metalloligand, which can potentially coordinate to other metals *via* the phosphine groups. Thus, complex **2** was subjected to reactivity tests with [Au(tht)Cl] and [Au(tht)C₆F₅] at room temperature in THF, which resulted in the formation of complexes [Au(X)Ph₂PC≡CC(NDipp)₂Cu₂] (X = Cl (**5**), C₆F₅ (**6**)) as the heterobimetallic complexes with Cu^I and Au^I centres (Scheme 4).

During the reaction,^[54] noticeable changes in the colour were observed, transitioning from bright yellow to dark yellow, and the luminescent properties resembled those of the starting material.

To verify the molecular structure, SC-XRD analysis was conducted (Figure 3), revealing an Au–P bond length of 2.23(2) Å and 2.274(9) Å in **5** and **6**, respectively. The Cu–N distances are almost similar in both the complexes (**5**: 1.887(5) Å and 1.889(5) Å; **6**: 1.876(3) Å and 1.880(3) Å). Additionally, cuprophilic interactions were observed in both complexes with Cu–Cu separation of 2.552(13) Å (**5**) and 2.537(8) Å (**6**).^[35] The Au^I ion is linearly coordinated by the phosphine moiety with bond angles of P–Au–Cl: 175.9(7)° (**5**) and P–Au–C: 176.5(10)° (**6**). Furthermore, Cu^I is also bonded almost linearly to the N atoms of the amidinate ligands with N–Cu–N bond angles of 173.7(2)° (**5**) and 174.0(12)° (**6**). In the mass spectrum, molecular



Scheme 3. Synthesis of gold(I) amidinate complex **3** *via* two different synthetic routes

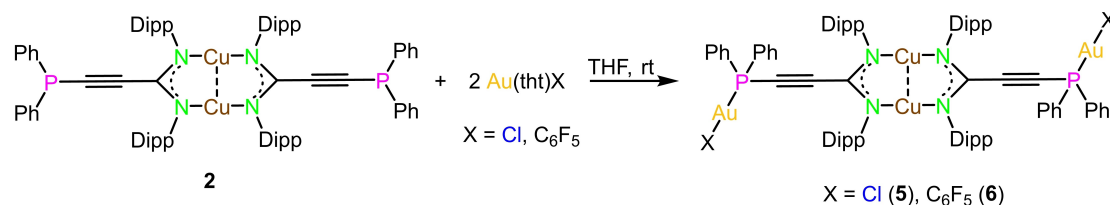
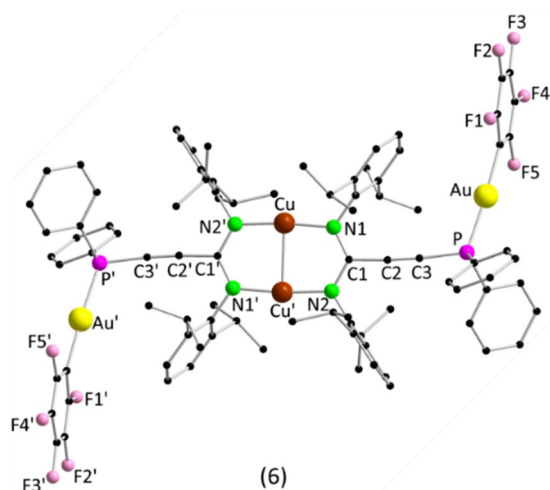
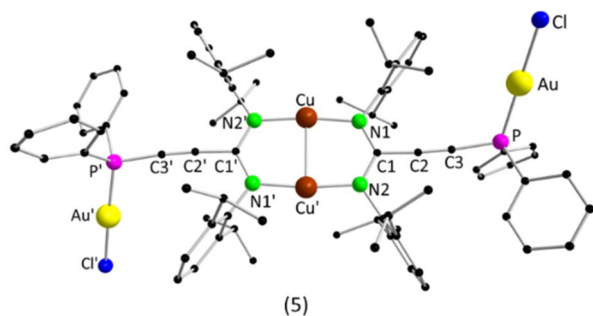
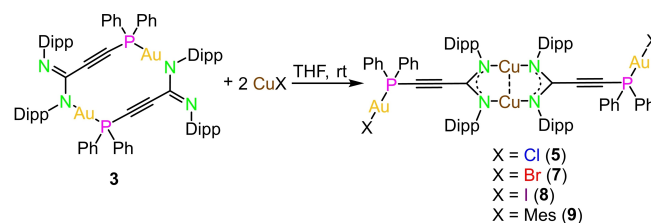
Scheme 4. Reactivity of complex 2 with Au(tht)Cl and Au(tht)C₆F₅.

Figure 3. Molecular structures of 5 (top) and 6 (bottom) in the solid state. Hydrogen atoms and non-coordinating solvents are omitted for clarity. Structural parameters are given in the ESI (Figure S45 and S46).

ion peaks at $m/z=1732.3630$ (5) and 1996.4052 (6) were observed for both compounds.

The additional confirmation of the product's identity was achieved through NMR analysis. Notably, a signal at $\delta=2.1$ ppm was observed in the $^{31}\text{P}\{^1\text{H}\}$ NMR spectrum for 5 and at $\delta=15.1$ ppm for 6, in contrast to the reactant's signal at $\delta=19.9$ ppm. These results collectively confirm the successful formation of heterobimetallic Cu^I–Au^I complexes 5 and 6.

Next, the order of the reaction was reversed wherein, the cyclic gold complex 3 was treated with various Cu^I salts. Overnight reactions of complex 3 with CuX (X=Cl, Br, I and mesityl) in THF at room temperature resulted in a significant rearrangement. As a result, complexes $[\{\text{Au}(\text{X})\text{Ph}_2\text{PC}\equiv\text{C}(\text{NDipp})_2\}_2\text{Cu}_2]$ (X=Cl (5), Br (7), I (8), Mes (9)) were obtained (Scheme 5), in which the same (amidinate)₂Cu₂ core structure as in 2 with the Au^I ions attached to P atoms are formed. In fact, compound 5 was obtained in both ways, using either 2 or 3 as



Scheme 5. Reactivity of complex 3 with different Cu(I) salts.

precursor. Compounds 5 and 7–9 were obtained in a good yield, ranging from 57–67% starting from the gold precursor 3. During the reactions, a consistent colour change from bright to dark yellow was observed for each product. Furthermore, when subjected to UV light, all of these products exhibited bright emission.

Compounds 7–9 were thoroughly characterized using standard analytical techniques (Figure 4). The molecular structures of these compounds were further elucidated through SC-XRD analysis. The analysis revealed an eight-membered ring at the centre of the molecule, containing two amidinate units and two copper atoms, which was also found in 2, 5 and 6. Additionally, the Cu–Cu distances were determined to be 2.569(14) Å, 2.526(9) Å, and 2.511(8) Å for compounds 7–9, respectively. These distances are consistent with the presence of cuprophilic interactions.^[36]

In the ^1H NMR spectra, slight differences were observed among the compounds. Notably, compound 9 displayed two expected additional sets of signals for the *o*- and *p*-methyl groups at $\delta=2.42$ and 2.24 ppm, respectively, as well as a distinct signal for the aromatic protons of the mesityl group. In contrast, significant differences were evident in the $^{31}\text{P}\{^1\text{H}\}$ NMR spectra. The chemical shifts observed for compounds 7–9 in the $^{31}\text{P}\{^1\text{H}\}$ NMR spectrum were $\delta=4.3$, 8.5, and 18.8 ppm, respectively. Additionally, the molecular ion peaks at $m/z=1820.2576$, 1916.2322 and 1900.6025 confirm the formation of complexes 7–9, respectively.

From the insights gained from previous reactions, where we observed the tendency of Cu^I to bond with N atoms of the amidinate ligand and Au^I to preferentially coordinate the phosphine group in accordance with Pearson's HSAB principle, we decided to attempt a one-pot reaction using all the basic constituents of compounds 5–9. In a one-pot reaction, we reacted the lithium salt 1 with Au(tht)Cl, {Au(tht)C₆F₅ for complex 6}, and a CuX precursor (where X=Cl (5), Br (7), I (8), mesityl (9)) at room temperature in THF (Scheme 6). Surprisingly, this one-pot approach led to a significant enhancement

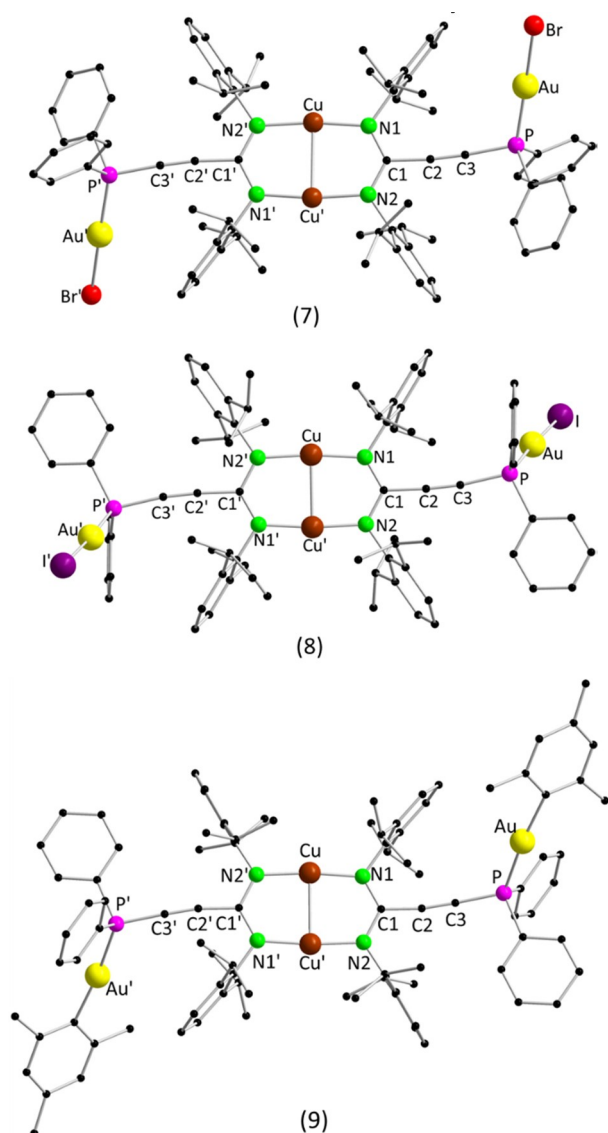


Figure 4. Molecular structures of **7**, **8** and **9** in the solid state. Hydrogen atoms and non-coordinating solvents are omitted for clarity. Structural parameters are given in the ESI (Figure S47, S48 and S49).

of the yields of the target products, which were now found to be around 60–85%, noticeably higher when compared to the yields obtained in the step-wise procedure. The success of this one-pot reaction strategy not only streamlined the synthesis process but also improved the overall yields of the desired compounds **5–9**. This efficient approach provided a valuable

method for obtaining these heterobimetallic complexes in higher yields and has opened up new possibilities for further exploring the reactivity of such compounds.

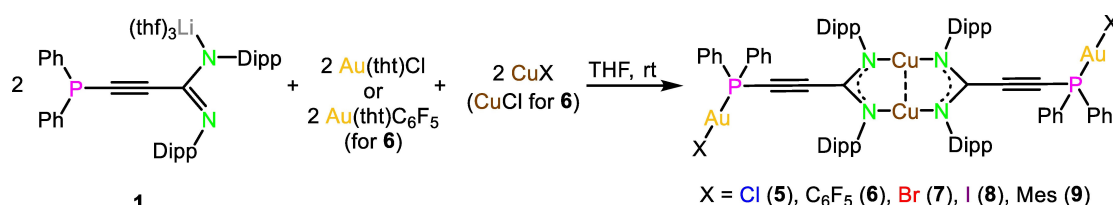
Photophysical Properties

The lithium salt **1** and the gold(I) complex **3** do not exhibit any significant luminescence in the solid state as well as in solution. The blue shift of the absorption onset of complex **3** (Figure S50) and its non-luminescence behaviour can be attributed to the absence of excited states resulting from metallophilic interactions.^[59–60] The luminescent metalloligand **2** and the bimetallic complexes **5–9** were investigated for their photophysical properties both in solution and in the solid state, and their PL data are tabulated in Table 1.

The PL emission and excitation (PLE) spectra of the metalloligand **2** are displayed in Figure 5. The emission profile of **2** exhibits a vibronic structure at 77 K both in solution and in the solid state with emission maxima at 490 nm. The decrease in PL intensity of the compound with increasing temperature is relatively higher in solution when compared to the solid state. This could be a consequence of enhanced thermally activated non-radiative processes in solution, resulting in a lower emission intensity at room temperature. The excited states of the metalloligand **2** decay with 71 μ s and 47 μ s at room temperature in solution and solid state, respectively, indicating phosphorescence behaviour.

The bimetallic complexes **5**, **7** and **8**, which differ in terms of anionic halogen ligand (Cl, Br and I), show a rather similar excitation and emission spectra in the PL spectroscopy (Figure 6). The complexes exhibit excitation maxima at \sim 450 nm in DCM solutions. Additionally, the shape of the excitation spectra is dependent on the emission wavelengths. The emission profiles of these complexes feature vibronic structure at 77 K and are broad at room temperature. The emission maximum of these complexes is red-shifted when compared to the metalloligand **2**.

The PL intensity of these complexes strongly decrease with increasing temperature. A clear trend for the changes in emission intensity can be observed among these complexes, wherein the emission intensity decreases on moving from complex **5** with chlorine group to bromine (**7**) and iodine (**8**) analogues (Figure 6a). This decrease in PL intensity on moving down the halogen group is mainly a consequence of the heavy atom effect.^[61] The solid state measurements of the complexes were carried out for the polycrystalline samples (Figure 6b). The

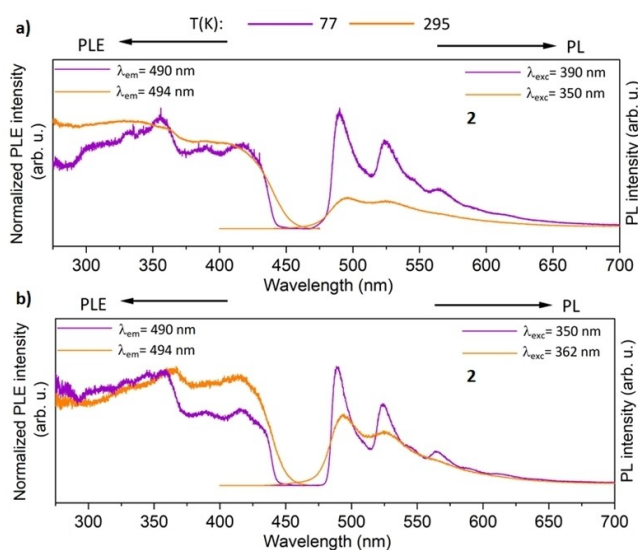


Scheme 6. One pot synthesis of compounds **5–9**.

Table 1. Photophysical data of the metalloligand **2** and the bimetallic complexes **5–9** in solution and in the solid state.

Compound	Solution				Solid				QY (%)
	Lifetimes of the excited state		λ_{max} (nm)		Lifetimes of the excited state		λ_{max} (nm)		
	rt	77 K	rt	77 K	rt	77 K	rt	77 K	
	(μs)	(μs)			(μs)	(μs)			
2	71	153	490	490	47	144	490	490	9.3
5	–*	28	540	575	12	17	535	580	3.0
6	9	51	560	545	26	36	530, 565	530, 560	6.5
7	–*	20	570(br)	575	14	19	570	580	5.9
8	8	39	570(br)	575	15	25	570	580	6.4
9	–*	33	550	535	21	24	535	560	7.7

*– The measured values are below the detection limit of our detector.

**Figure 5.** Normalized photoluminescence excitation (PLE) and emission (PL) spectra of the metalloligand **2** at room temperature and 77 K a) in benzene, b) in the solid state. PLE and PL spectra were recorded at the depicted wavelengths (λ_{em} and λ_{exc}).

emission maxima of these compounds in solid state are slightly red-shifted at 77 K with respect to the solutions. The emission profiles are similar to that of the solution. However, the PL intensity of the complexes follows an opposite trend with respect to the solutions, i.e., $8 > 7 > 5$ (Figure 6b). The gold(I) iodo complex **8** retains PL intensity comparable to 77 K, whereas its chloro and bromo analogues exhibit a decrease in emission intensity at room temperature. The opposite trend might be due to predominant role of molecular packing effects in the solid state in comparison to the heavy atom effect.

The gold(I) complex **9** with mesityl ancillary ligand features a broad emission spectrum both in solution and in the solid state (Figure 7). The PL intensity of the compound declines with increase in temperature. In contrast, complex **6** in the solid state retains its emission efficiency comparable to 77 K. The presence of fluorine groups in complex **6** led to a blue-shift in the emission spectra when compared to the other bimetallic

complexes, which is in line with previously reported observations.^[62]

It is also noteworthy that for complex **6** and **9**, the emission profile is independent of the excitation wavelengths (Figure 7). The PL of complexes **6** and **9** is also phosphorescence as indicated by microsecond-long emission decays of the excited states. Quantum yields of the complexes were determined to be less than 10% at room temperature. The bimetallic complexes exhibit comparatively lower quantum efficiency and the photoactive excited states decay rapidly when compared to the metalloligand **2** (Table 1). This enhanced non-radiative quenching of luminescence for the heterobimetallic complexes **5–9** is likely to arise from additional rotational degrees of freedom introduced by a second metal.^[63] These heterobimetallic complexes with absorption in the visible region and low-energy emission can be potential candidates for photocatalytic applications.

Conclusions

The syntheses of phosphine acetylide amidinate stabilized copper(I) and gold(I) heterobimetallic complexes were successfully established. Starting with the synthesis of the lithium amidinate $[\{\text{Ph}_2\text{PC}\equiv\text{CC}(\text{NDipp})_2\}\text{Li}(\text{thf})_3]$ (**1**), the copper and gold complexes $[\{\text{Ph}_2\text{PC}\equiv\text{CC}(\text{NDipp})_2\}_2\text{Cu}_2]$ (**2**) and $[\{\text{Ph}_2\text{PC}\equiv\text{CC}(\text{NDipp})_2\}_2\text{Au}_2]$ (**3**) were obtained, which exhibit significantly different molecular structures due to varying coordination modes. However, further reaction of the copper complex **2** with Au^{I} compounds or vice versa reaction of the gold complex **2** with Cu^{I} compounds resulted in the same structural motif $[\{(\text{AuX})\text{Ph}_2\text{PC}\equiv\text{CC}(\text{NDipp})_2\}_2\text{Cu}_2]$ ($\text{X} = \text{Cl}, \text{C}_6\text{F}_5, \text{Br}, \text{I}, \text{Mes}$). Furthermore, complexes **5–9** can also be obtained by one-pot reaction of **1**, $\text{Au}(\text{tht})\text{Cl}/\text{Au}(\text{tht})\text{C}_6\text{F}_5$ and CuX in an equimolar ratio. Complex **2** and the bimetallic complexes **5–9** emit yellow phosphorescence due to the presence of cuprophilic interactions and were investigated for their photophysical properties both in solution and in the solid state. For all these luminescent complexes, the emission maximum lies in the range of 490–580 nm.

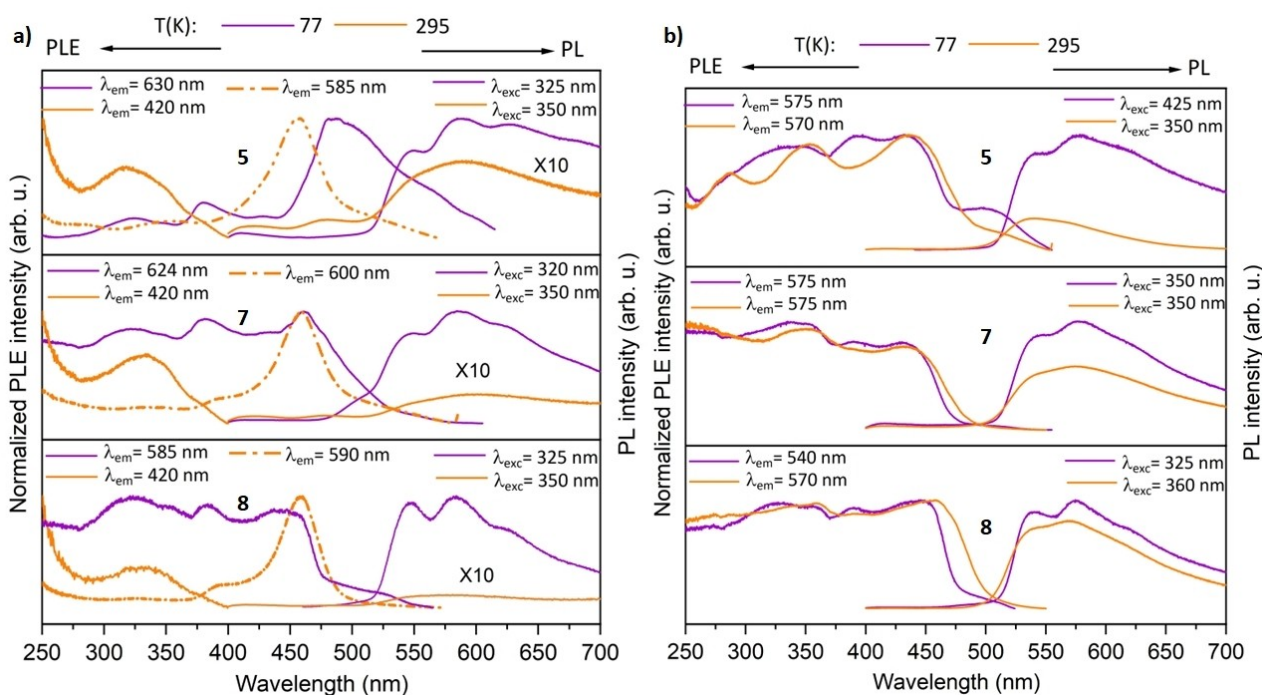


Figure 6. Normalized photoluminescence excitation (PLE) and emission (PL) spectra of bimetallic complexes **5**, **7**, and **8** in a) DCM solutions and b) solid state at room temperature and 77 K. PLE and PL spectra were recorded at the depicted wavelengths (λ_{em} and λ_{exc}).

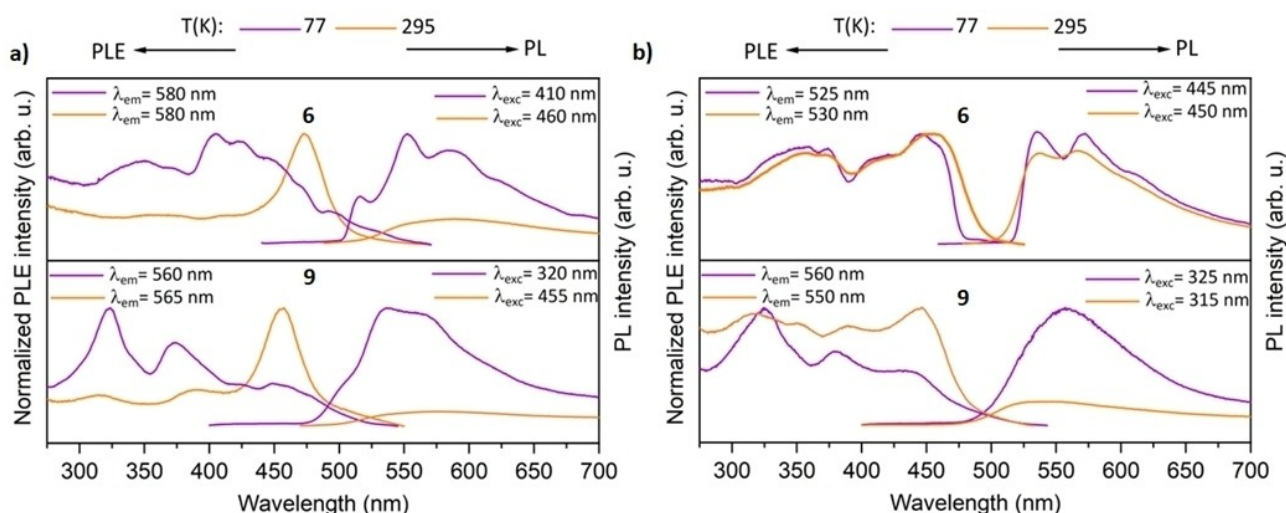


Figure 7. Normalized photoluminescence excitation (PLE) and emission (PL) spectra of bimetallic complexes **6** and **9** in a) DCM solutions and b) solid state at room temperature and 77 K. PLE and PL spectra were recorded at the depicted wavelengths (λ_{em} and λ_{exc}).

Experimental Section

The syntheses and characterization of all compounds, NMR, HRES-MS, IR, absorption spectra and PL spectra as well as X-ray crystallography details are given in the Supporting Information.

Deposition Numbers 2349634 (for **1**), 2349635 (for **3**), 2349636 (for **5**), 2349637 (for **6**), 2349638 (for **7**), 2349639 (for **8**) and 2349640 (for **9**) contain the supplementary crystallographic data for this paper. These data are provided free of charge by the joint Cambridge Crystallographic Data Centre and Fachinformationszentrum Karlsruhe Access Structures service.

Acknowledgements

S, VRN, and PWR acknowledges GRK 2039 Molecular Architectures for Fluorescent Cell Imaging for the financial support. PWR acknowledges Deutsche Forschungsgemeinschaft for support within the project 540378534, RO 2008/22-1. Open Access funding enabled and organized by Projekt DEAL.

Conflict of Interests

The authors declare no conflict of interest.

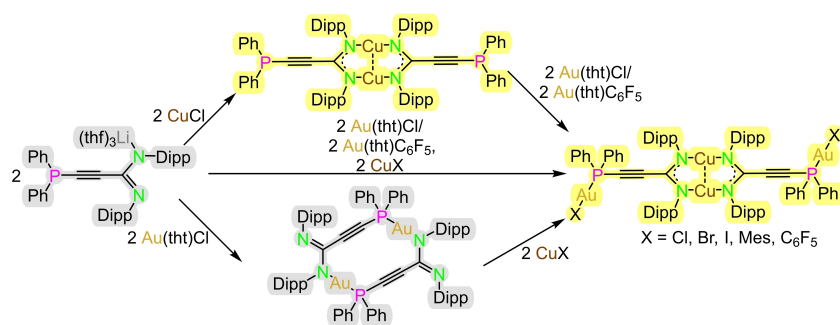
Data Availability Statement

The data that support the findings of this study are available in the supplementary material of this article.

Keywords: Coinage metals · Amidinate · Orthogonal ligand · Heterobimetallic complexes · Photoluminescence

- [1] D. Das, S. S. Mohapatra, S. Roy, *Chem. Soc. Rev.* **2015**, *44*, 3666–3690.
- [2] B. G. Cooper, J. W. Napoline, C. M. Thomas, *Catal. Rev.* **2012**, *54*, 1–40.
- [3] H. Xu, R. Chen, Q. Sun, W. Lai, Q. Su, W. Huang, X. Liu, *Chem. Soc. Rev.* **2014**, *43*, 3259–3302.
- [4] N. Desbois, S. Pacquelet, A. Dubois, C. Michelin, C. P. Gros, *Beilstein J. Org. Chem.* **2015**, *11*, 2202–2208.
- [5] L. Peña, C. Jiménez, R. Arancibia, A. Angeli, C. T. Supuran, *J. Inorg. Biochem.* **2022**, *232*, 111814.
- [6] M. Böhmer, G. Guisado-Barríos, F. Kampert, F. Roelfes, T. T. Y. Tan, E. Peris, F. E. Hahn, *Organometallics* **2019**, *38*, 2120–2131.
- [7] W. Zhou in *Synthesis and Catalytic Application of Heterobimetallic Complexes, Vol. Doctor of Philosophy* Brandeis University, **2013**.
- [8] M. Hardy, N. Struch, F. Topić, G. Schnakenburg, K. Rissanen, A. Lützen, *Inorg. Chem.* **2018**, *57*, 3507–3515.
- [9] H.-K. Yip, H.-M. Lin, Y. Wang, C.-M. Che, *J. Chem. Soc., Dalton Trans.* **1993**, 2939–2944.
- [10] H.-K. Yip, H.-M. Lin, K.-K. Cheung, C.-M. Che, Y. Wang, *Inorg. Chem.* **1994**, *33*, 1644–1651.
- [11] C. Uhlmann, T. J. Feuerstein, T. P. Seifert, A. P. Jung, M. T. Gamer, R. Köppe, S. Lebedkin, M. M. Kappes, P. W. Roesky, *Dalton Trans.* **2022**, *51*, 10357–10360.
- [12] V. W.-W. Yam, K. M.-C. Wong, *Chem. Commun.* **2011**, *47*, 11579–11592.
- [13] R. G. Pearson, *J. Am. Chem. Soc.* **1963**, *85*, 3533–3539.
- [14] R. G. Pearson, *J. Chem. Educ.* **1968**, *45*, 581.
- [15] R. G. Pearson, *J. Chem. Educ.* **1968**, *45*, 643.
- [16] V. J. Catalano, M. A. Malwitz, A. O. Etogo, *Inorg. Chem.* **2004**, *43*, 5714–5724.
- [17] V. J. Catalano, A. L. Moore, *Inorg. Chem.* **2005**, *44*, 6558–6566.
- [18] M. J. Calhorda, C. Ceamanos, O. Crespo, M. C. Gimeno, A. Laguna, C. Larraz, P. D. Vaz, M. D. Villacampa, *Inorg. Chem.* **2010**, *49*, 8255–8269.
- [19] C. E. Strasser, V. J. Catalano, *Inorg. Chem.* **2011**, *50*, 11228–11234.
- [20] E. Hobbollahi, M. List, B. Hupp, F. Mohr, R. J. F. Berger, A. Steffen, U. Monkowius, *Dalton Trans.* **2017**, *46*, 3438–3442.
- [21] C. Kaub, S. Lebedkin, S. Bestgen, R. Köppe, M. M. Kappes, P. W. Roesky, *Chem. Commun.* **2017**, *53*, 9578–9581.
- [22] C. Kaub, S. Lebedkin, A. Li, S. V. Kruppa, P. H. Strebert, M. M. Kappes, C. Riehn, P. W. Roesky, *Chem. Eur. J.* **2018**, *24*, 6094–6104.
- [23] V. R. Naina, F. Krätschmer, P. W. Roesky, *Chem. Commun.* **2022**, *58*, 5332–5346.
- [24] W.-H. Chan, K.-K. Cheung, T. C. W. Mak, C.-M. Che, *J. Chem. Soc., Dalton Trans.* **1998**, 873–874.
- [25] O. Crespo, E. J. Fernández, M. Gil, M. Concepción-Gimeno, P. G. Jones, A. Laguna, J. M. López-de-Luzuriaga, M. Elena Olmos, *J. Chem. Soc. Dalton Trans.* **2002**, 1319–1326.
- [26] V. J. Catalano, J. M. López-de-Luzuriaga, M. Monge, M. E. Olmos, D. Pascual, *Dalton Trans.* **2014**, *43*, 16486–16497.
- [27] T. P. Seifert, S. Bestgen, T. J. Feuerstein, S. Lebedkin, F. Krämer, C. Fengler, M. T. Gamer, M. M. Kappes, P. W. Roesky, *Dalton Trans.* **2019**, *48*, 15427–15434.
- [28] A. Márquez, E. Ávila, C. Urbaneja, E. Álvarez, P. Palma, J. Cámpora, *Inorg. Chem.* **2015**, *54*, 11007–11017.
- [29] N. Mirzadeh, S. H. Privér, A. J. Blake, H. Schmidbaur, S. K. Bhargava, *Chem. Rev.* **2020**, *120*, 7551–7591.
- [30] V. W.-W. Yam, V. K.-M. Au, S. Y.-L. Leung, *Chem. Rev.* **2015**, *115*, 7589–7728.
- [31] S. Raju, H. B. Singh, R. J. Butcher, *Dalton Trans.* **2020**, *49*, 9099–9117.
- [32] H. Schmidbaur, A. Schier, *Chem. Soc. Rev.* **2012**, *41*, 370–412.
- [33] F. Scherbaum, A. Grohmann, G. Müller, H. Schmidbaur, *Angew. Chem. Int. Ed.* **1989**, *28*, 463–465.
- [34] H. Schmidbaur, *Gold Bull.* **1990**, *23*, 11–21.
- [35] M. Jansen, *Angew. Chem. Int. Ed.* **1987**, *26*, 1098–1110.
- [36] N. V. S. Harisomayajula, S. Makovetskyi, Y.-C. Tsai, *Chem. Eur. J.* **2019**, *25*, 8936–8954.
- [37] H. L. Hermann, G. Boche, P. Schwerdtfeger, *Chem. Eur. J.* **2001**, *7*, 5333–5342.
- [38] H. Schmidbaur, A. Schier, *Angew. Chem. Int. Ed.* **2015**, *54*, 746–784.
- [39] M. Jansen, *J. Less-Common Met.* **1980**, *76*, 285–292.
- [40] V. W.-W. Yam, E. Chung-Chin Cheng in *Photochemistry and photophysics of coordination compounds II, Vol. 281* (Ed. S. C. a. A. B. V. Balzani), Springer, Berlin, Heidelberg, **2007**.
- [41] S. Bestgen, M. T. Gamer, S. Lebedkin, M. M. Kappes, P. W. Roesky, *Chem. Eur. J.* **2015**, *21*, 601–614.
- [42] Z. Li, S. T. Barry, R. G. Gordon, *Inorg. Chem.* **2005**, *44*, 1728–1735.
- [43] A. C. Lane, M. V. Vollmer, C. H. Laber, D. Y. Melgarejo, G. M. Chiarella, J. P. Fackler Jr., X. Yang, G. A. Baker, J. R. Walensky, *Inorg. Chem.* **2014**, *53*, 11357–11366.
- [44] A. C. Lane, C. L. Barnes, W. E. Antholine, D. Wang, A. T. Fiedler, J. R. Walensky, *Inorg. Chem.* **2015**, *54*, 8509–8517.
- [45] N. V. S. Harisomayajula, B.-H. Wu, D.-Y. Lu, T.-S. Kuo, I. C. Chen, Y.-C. Tsai, *Angew. Chem. Int. Ed.* **2018**, *57*, 9925–9929.
- [46] N. Nebra, C. Lescot, P. Dauban, S. Mallet-Ladeira, B. Martin-Vaca, D. Bourissou, *Eur. J. Org. Chem.* **2013**, *2013*, 984–990.
- [47] S. C. Rathnayaka, S. V. Lindeman, N. P. Mankad, *Inorg. Chem.* **2018**, *57*, 9439–9445.
- [48] S. C. Rathnayaka, C.-W. Hsu, B. J. Johnson, S. J. Iniguez, N. P. Mankad, *Inorg. Chem.* **2020**, *59*, 6496–6507.
- [49] B. J. Johnson, W. E. Antholine, S. V. Lindeman, N. P. Mankad, *Chem. Commun.* **2015**, *51*, 11860–11863.
- [50] V. R. Naina, A. K. Singh, P. Rauthe, S. Lebedkin, M. T. Gamer, M. M. Kappes, A.-N. Unterreiner, P. W. Roesky, *Chem. Eur. J.* **2023**, *29*, e202300497.
- [51] R. P. Herrera, M. C. Gimeno, *Chem. Rev.* **2021**, *121*, 8311–8363.
- [52] T. J. Feuerstein, M. Poß, T. P. Seifert, S. Bestgen, C. Feldmann, P. W. Roesky, *Chem. Commun.* **2017**, *53*, 9012–9015.
- [53] E. V. Grachova, *Russ. J. Gen. Chem.* **2019**, *89*, 1102–1114.
- [54] T. J. Feuerstein, T. P. Seifert, A. P. Jung, R. Müller, S. Lebedkin, M. M. Kappes, P. W. Roesky, *Chem. Eur. J.* **2020**, *26*, 16676–16682.
- [55] M. Dahlen, E. H. Hollesen, M. Kehry, M. T. Gamer, S. Lebedkin, D. Schooss, M. M. Kappes, W. Klopfer, P. W. Roesky, *Angew. Chem. Int. Ed.* **2021**, *60*, 23365–23372.
- [56] M. Dahlen, M. Kehry, S. Lebedkin, M. M. Kappes, W. Klopfer, P. W. Roesky, *Dalton Trans.* **2021**, *50*, 13412–13420.
- [57] M. Dahlen, T. P. Seifert, S. Lebedkin, M. T. Gamer, M. M. Kappes, P. W. Roesky, *Chem. Commun.* **2021**, *57*, 13146–13149.
- [58] H. Hao, T. Bagnol, M. Pucheault, L. L. Schafer, *Org. Lett.* **2021**, *23*, 1974–1979.
- [59] V. W.-W. Yam, T.-F. Lai, C.-M. Che, *J. Chem. Soc., Dalton Trans.* **1990**, 3747–3752.
- [60] A. Chakraborty, J. C. Deaton, A. Haefele, F. N. Castellano, *Organometallics* **2013**, *32*, 3819–3829.
- [61] A. Ghodbane, N. Saffon, S. Blanc, S. Fery-Forgues, *Dyes Pigm.* **2015**, *113*, 219–226.
- [62] Y. Chen, C. Liu, L. Wang, *Tetrahedron* **2019**, *75*, 130686.
- [63] J. Ma, J. Schaab, S. Paul, S. R. Forrest, P. I. Djurovich, M. E. Thompson, *J. Am. Chem. Soc.* **2023**, *145*, 20097–20108.

Manuscript received: April 29, 2024
Accepted manuscript online: May 17, 2024
Version of record online: ■■■, ■■■



Luminescent tetranuclear heterobimetallic complexes: Heterobimetallic Cu^I/Au^I complexes with phosphine acetylide amidinate ligand were syn-

thesized by using different reaction pathways. These complexes are found to be luminescent and differ in terms of ancillary ligands at Au^I centre.

Shubham, Dr. V. R. Naina,
Prof. Dr. P. W. Roesky*

1 – 9

Luminescent Tetranuclear Copper(I) and Gold(I) Heterobimetallic Complexes: A Phosphine Acetylide Amidinate Orthogonal Ligand Framework for Selective Complexation

